J. Fluid Mech. (1984), *vol.* 149, *pp.* 355–373
Printed in Great Britain

The interaction region of a turbulent plane jet

By L. W. B. BROWNE, R. A. ANTONIA AND A. J. CHAMBERS
Department of Mechanical Engineering, University of Newcastle, N.S.W., 2308, Australia

(Received 3 November 1983 and in revised form 6 July 1984)

All three velocity fluctuations and the temperature fluctuation have been measured in a slightly heated turbulent plane jet. Attention is focused on the interaction region of the flow, which is situated between the location where the two mixing layers nominally merge and that which corresponds to approximate self-preservation.

For the jet considered here the mixing-layer structures are symmetrical with respect to the centreline, and when they meet in the interaction region the redistribution of turbulence quantities is dramatic. This redistribution is examined in detail. Also examined is the effect of the generation, in the interaction region, of new structures, asymmetric with respect to the centreline, which evolve into the self-preserving flow region downstream.

Turbulence parameters, such as the turbulent Prandtl number, probability density functions, skewness and flatness factors, are also presented, primarily to guide computer simulations of this flow. The superposition procedure of Weir, Wood & Bradshaw (1981), which assumes that the turbulence structure of each mixing layer is not significantly altered by the interaction, is not appropriate to the present flow.

1. Introduction

There have been several experimental investigations of a turbulent plane jet exhausting into still air or into a coflowing free stream. Most of these have provided a wide range of measurements of turbulence quantities in either the self-preserving (or approximately self-preserving) mixing layers or in the approximately self-preserving flow well downstream of the nozzle (e.g. Bradbury 1965; Heskestad 1965; Gutmark & Wygnanski 1976; Everitt & Robins 1978). Several studies have focused on the three-dimensionality of the flow that issues from a rectangular nozzle. Some of these have been of an experimental nature (e.g. Trentacoste & Sforza 1967; Foss & Jones 1968; Sfeir 1979; Sforza and Stasi 1979; Krothapalli, Baganoff & Karamcheti 1981; Quinn, Pollard & Masters 1983); others of a modelling (e.g. Abramovich 1982) or computational nature (e.g. McGuirk & Rodi 1977). Other aspects that have been considered include the effect of initial conditions (e.g. Flora & Goldschmidt 1969; Hussain & Clark 1977; Goldschmidt & Bradshaw 1981) or room turbulence (Bradshaw 1977). More recently, attention has turned (Mumford 1982; Oler & Goldschmidt 1981; Antonia *et al.* 1983*b*) towards identifying the presence and properties of the organized large-structure of the flow, primarily through space–time correlation measurements. On the basis of flow-visualization results and quantitative measurements, Goldschmidt, Moallemi & Oler (1983) have suggested that a pattern of spanwise eddies, somewhat reminiscent of a Kármán vortex street, accounts for the flapping-like motion of the flow and for the regions of flow reversal which occur in the outer part of the jet.

One region of the flow that has been largely ignored, both experimentally and

computationally, is that located between the point where the opposite mixing layers meet and the point where the flow becomes approximately self-preserving. Although the location of neither point is precisely defined (it depends, among other things, on initial conditions at the nozzle), this region may be assumed to fall roughly in the range $3–5 \lesssim x/d \lesssim 20–40$. It is referred to here as the interaction region. Weir & Bradshaw's (1975) conditional measurements, made possible by marking one of the mixing layers with temperature, showed that the turbulence structure of each layer is significantly altered by interaction with the other. Weir, Wood & Bradshaw (1981) found that the behaviour of third-order moments, which affect the transport of the Reynolds stress, is significantly changed by the interaction, but the change was primarily confined to near the centreline region. These authors noted, however, that a calculation method using the superposition procedure, introduced originally by Bradshaw, Dean & McEligot (1973) for interacting shear layers in a duct flow, yielded satisfactory agreement with experiment. More recently Antonia *et al.* (1983*b*) showed that the counter-rotating spanwise structures† which alternate on opposite sides of the centreline and which feature prominently in the nearly self-preserving region of the flow have their origin in the interaction region. Upstream of this origin and in the mixing layers, the flow structure was significantly different from that downstream of the interaction region.

In view of the above remarks, it seemed important to consider the evolution of turbulence quantities, such as the Reynolds stresses and heat fluxes, throughout the interaction region and to explain this evolution in the light of the flow structure inferred from space–time correlations. In the investigation of Weir, Wood & Bradshaw (1981) only moments derived from the velocity fluctuations u and v were considered. In the present paper all three velocity fluctuations have been measured in addition to the temperature fluctuation. Several structural parameters of the turbulence, which are dimensionless ratios of turbulence quantities, have been calculated for the interaction region.

2. Experimental description and conditions

Air is supplied to the nozzle of the jet (width $d = 12.7$ mm, height = 250 mm) by a centrifugal squirrel-cage blower via a 25 cm × 25 cm × 2 m duct, screens and a 20:1 two-dimensional contraction. The jet is heated with 1 kW electrical coil elements distributed across the duct immediately downstream of the blower. An endplate (0.25 × 0.25 m) was fixed at the nozzle exit plane and confining horizontal panels (0.7 × 1.1 m) were installed (see inset figure 1) downstream of the nozzle exit plane. A more detailed description of the plane jet rig has been given in Antonia *et al.* (1983*a*).

The velocity fluctuations and temperature fluctuation were measured with an X-probe/cold-wire arrangement. The hot wires (5 μm Pt–10% Rh, 0.6 mm length) were mounted in the horizontal (x, y)-plane (see figure 1 for definition of coordinate axes) with a separation of about 0.5 mm. The 0.63 μm cold wire (Pt–10% Rh, 0.6 mm length) was located at about 0.5 mm upstream of the centre of the X-probe, othogonally to the X-probe plane. The hot wires were operated with constant-temperature anemometers at a resistance ratio of 1.8, while the cold wire was operated in a constant-current (0.1 mA) circuit. Voltages from the wires were digitized on a PDP 11/34 computer. The digitized hot-wire voltages were converted to velocity values, allowing for the effects of temperature. Probability density functions of u,

† A model for these structures was proposed by Oler & Goldschmidt (1982).

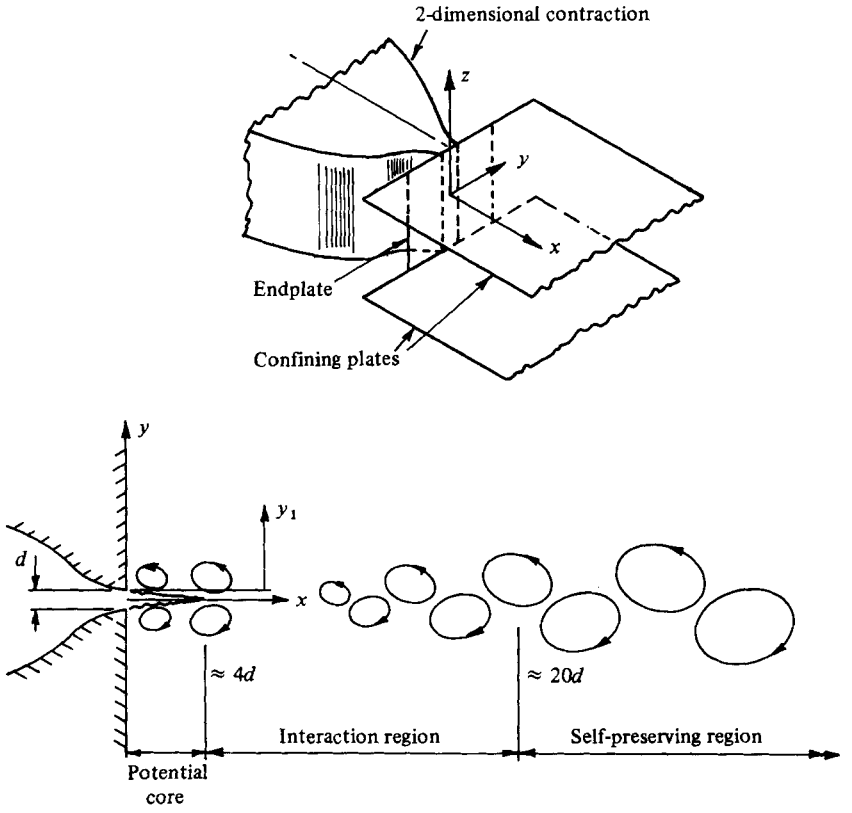

FIGURE 1. Coordinate system and simplified view of structures.

v, θ, average Reynolds stresses and average heat fluxes were calculated from digital records of approximately 60 s duration.

The mean velocity U in the x-direction and temperature T were obtained from the X-wire and cold-wire voltages respectively. The X-probe was calibrated for speed and yaw, for angles in the range $-25°-+25°$ in steps of 5°, at the nozzle exit plane. The temperature sensitivity of the cold wire was also determined at the nozzle exit. For the velocity calibration, a Pitot tube was connected to a Furness micromanometer with a resolution of 0.01 mm water. For the temperature calibration, a 10 Ω platinum resistance thermometer was operated with a Leeds and Northrup 8078 temperature bridge. The accuracy of mean temperature was estimated to be ± 0.01 °C. A data logger consisting of a data-acquisition system (HP3497A) and a desktop computer (HP85) was used for processing the calibration information and monitoring the performance of all three wires during the experiment.

The measurements were made for nominal values of U_j, the exit jet velocity, and T_j, the exit jet temperature relative to ambient, of 9 m s^{-1} and 25 °C respectively. The boundary layers were laminar at the nozzle exit, the measured velocity distributions in the boundary layers on opposite lips of the nozzle closely following the Blasius distribution. Values of u'/U_j and θ'/T_j (a prime denotes an r.m.s. value) measured at $y = 0$ and $x = 0$ are equal to about 0.001. Measurements of U, T, $\overline{uv}$ and $\overline{v\theta}$ indicated that the mixing layers were approximately self-preserving at $x/d \approx 4$.

Estimates of the random component of uncertainty for quantities measured with the X-probe/cold-wire arrangement are shown in table 1. These estimates were

$$U = \pm 1.5\%, \quad T = \pm 3\%$$
$$u' = \pm 3\%, \quad v', w' = \pm 4\%, \quad \theta' = \pm 4\%$$
$$\overline{uv} = \pm 7\%, \quad \overline{v\theta} = \pm 12\%$$
$$\partial T/\partial U = \pm 3\%, \quad Pr_t = \pm 14\%$$

TABLE 1. Estimated uncertainties of quantities measured with the X-probe/cold-wire arrangement

inferred from estimated inaccuracies in the calibration data and from the observed scatter in the measurements. The uncertainty in the turbulent Prandtl number Pr_t was calculated from the tabulated uncertainties in $\overline{uv}$ and $\overline{v\theta}$ and an uncertainty in $\partial T/\partial U$ of about $\pm 3\%$. An indirect measure of the reliability of $\overline{uv}$ and $\overline{v\theta}$ in the nearly self-preserving flow region was obtained by calculating (Browne & Antonia 1983) these quantities via the mean momentum and mean enthalpy equations. The agreement between measurement and calculation was found to be within the estimated experimental uncertainty.

3. General description of the flow and coordinate system

The large-scale structures that exist in this particular flow have been delineated by measurements of space–time correlations of longitudinal and normal velocity fluctuations and of temperature fluctuations and have been reported in Antonia *et al.* (1983*b*). In summary (figure 1), spanwise counter-rotating structures that are symmetrical about the centreline exist in the mixing layers prior to the start of the interaction region. Counter-rotating spanwise structures appear alternately on opposite sides of the jet centreline approximately halfway down the interaction region. Structures grow and appear to dominate the self-preserving region, downstream of the interaction region. The results obtained for the interaction region and which are presented here are interpreted whenever possible, within the framework of this general description.

The coordinate η ($\equiv y/L_u$, where L_u is the y-value where the local mean streamwise velocity is half the centreline mean velocity) is used for presenting the majority of the results. This coordinate is strictly relevant only to the nearly self-preserving region downstream of the interaction region. However, the use of η enables the rapidity with which turbulent quantities in the interaction region approach self-preservation to be assessed. Another choice of coordinate could have been y_1/x, where y_1 is measured from the nozzle lip (figure 1). This coordinate is strictly relevant to the mixing layer, and, when used in the interaction region (e.g. Weir *et al.* 1981), indicates the degree of departure from the self-preserving mixing layer. Clearly either η or y_1/x would be adequate for the purpose of presenting the evolution of turbulence quantities in the interaction region.

The largest value of η shown in all subsequent figures is 1.5, as the accuracy of the data obtained with the X-probe/cold-wire configuration is estimated to be poor beyond this value of η. Flow reversal in the outer region of a plane jet has been established by Kotsovinos (1975) using a laser velocimeter, Moallemi & Goldschmidt (1981) using a smoke-wire technique and Goldschmidt *et al.* (1983) using a hot-wire/cold-wire arrangement. In the present work, flow reversal is detected by the cold wire, which is located upstream of the hot wires and therefore senses their thermal

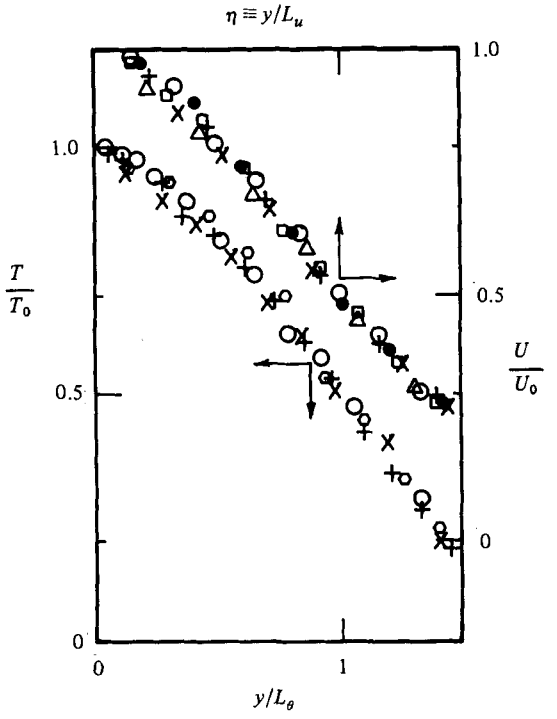

FIGURE 2. Mean-velocity and mean-temperature profiles: △, $x/d = 5$; ×, 7; +, 8; ●, 9; ○, 15; □, 20; ○, 40.

wakes. Detection of reversed flow first occurs at $\eta \approx 1$ and is almost independent of location in the interaction region. The frequency of reversal is sufficiently high at $\eta \approx 1.2$ to place in doubt the validity of the data beyond this point.

4. Mean-flow field

Mean-velocity and mean-temperature profiles for $x/d \geqslant 5$ are shown in figure 2. For normalization purposes the centreline mean velocity U_0, the centreline mean temperature T_0 and the lengthscales L_u and L_θ, where L_θ is the value of y at which the local mean temperature is half the centreline mean temperature, have been used. For $x/d \gtrsim 5$, the dependence on x of L_u, L_θ, U_0 and T_0 has been described in Browne *et al.* (1983). For $x/d \gtrsim 20$, the dependence is given approximately by the following relations: $L_u/d = 0.104(x/d+5)$, $(U_j/U_0)^2 = 0.143(x/d+9)$ and $(T_j/T_0)^2 = 0.18\,(x/d+8)$. The ratio L_θ/L_u is approximately 1.23 for $x/d \gtrsim 20$. The mean-velocity and mean-temperature profiles (figure 2) indicate that similarity is satisfied almost at $x/d = 5$. This is consistent with the observation by Tennekes & Lumley (1972, p. 130) that measured mean-velocity profiles in a plane jet appear to be self-preserving beyond $x/d = 5$. It is also well known that mean-velocity profiles for a wide range of flows are not a sensitive indicator of self-preservation. The relatively large momentum in the mean-flow direction tends to inhibit any major redistribution of mean velocity or mean temperature by the large-scale structures. The evolution of turbulence quantities as the flow moves downstream provides a far more sensitive criterion for the establishment of self-preservation.

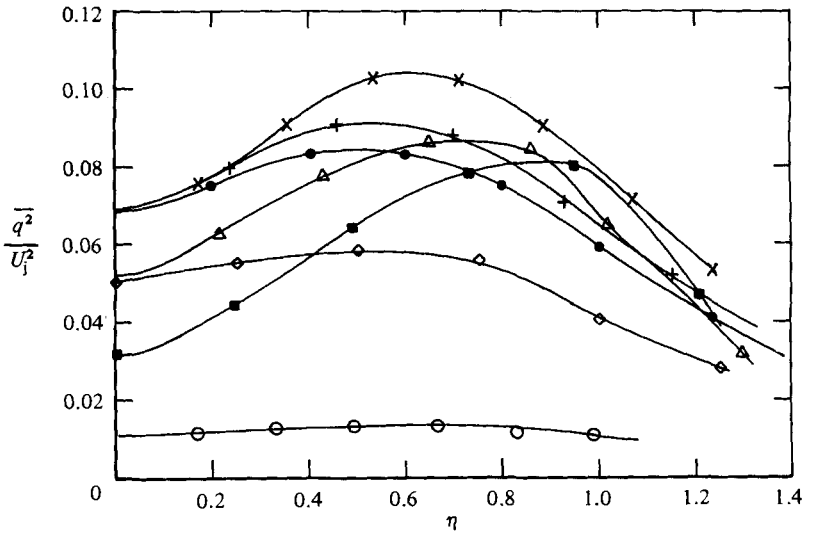

FIGURE 3. Distributions of $\overline{q^2}/U_j^2$ across the jet: ■, $x/d = 4$; ◇, 12; other symbols are as in figure 2.

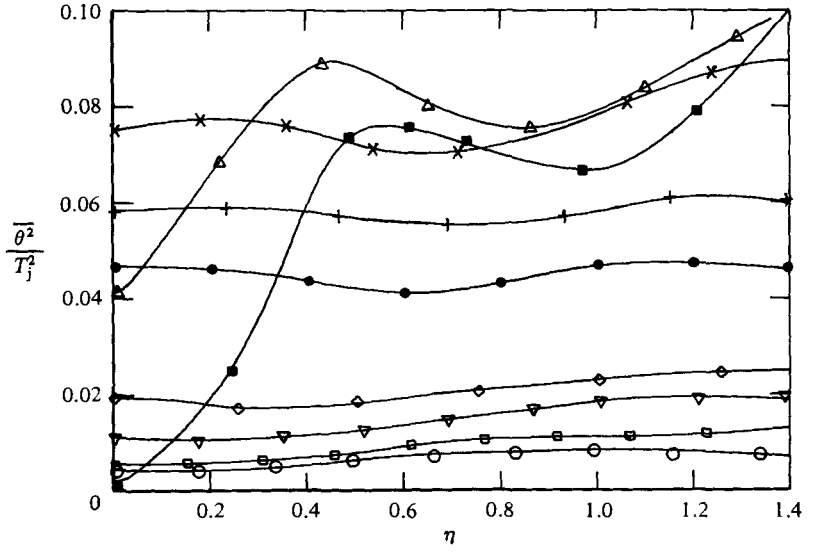

FIGURE 4. Distributions of $\overline{\theta^2}/T_j^2$ across the jet: ■, $x/d = 4$; ◇, 12; ▽, 14; other symbols are as in figure 2.

5. Reynolds stresses, r.m.s. temperature and heat flux

One of the most interesting features of the interaction region is the way in which the turbulence intensities redistribute across the jet as the flow moves downstream. Figures 3 and 4 show that, at the start of the interaction region ($x/d \approx 4$), the mean turbulent energy $\overline{q^2}$ and the mean-square temperature fluctuation $\overline{\theta^2}$ have distributions reflecting their generation by the interaction of the jet core flow with the surrounding air, i.e. the values are quite low on the centreline of the jet and quite high towards the edges of the jet. However, as the mixing-layer structures on either side of the potential core meet, the distributions of $\overline{q^2}$ and $\overline{\theta^2}$ change dramatically in a very short

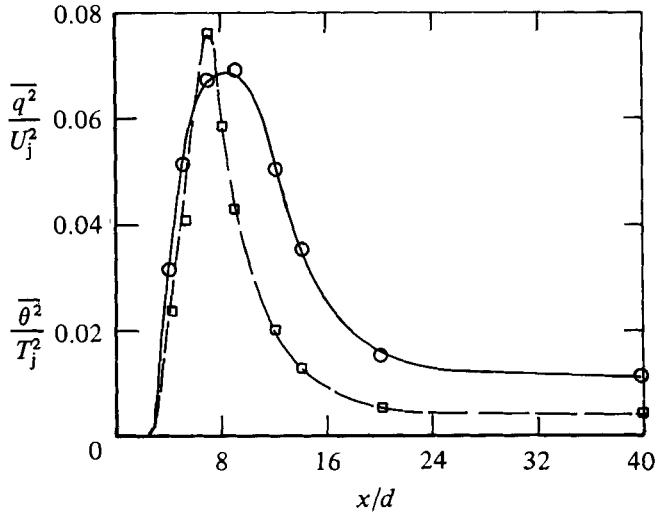

FIGURE 5. Centreline distributions of $\overline{q^2}$ and $\overline{\theta^2}$: ○, $\overline{q^2}/U_j^2$; □, $\overline{\theta^2}/T_j^2$.

distance. Figure 5, which shows the centreline values of $\overline{q^2}$ and $\overline{\theta^2}$, also highlights the rapid changes that occur in the interaction region. In figure 4, $\overline{\theta^2}$ is almost uniform across the jet by $x/d = 8$, while the redistribution (figure 3) of $\overline{q^2}$, although not as uniform as $\overline{\theta^2}$, is considerably increased in magnitude, particularly near the centreline. A possible description for the interaction between opposite mixing-layer structures may be in terms of a collision, as the changes that occur downstream of $x/d \approx 4$ are somewhat reminiscent of the very rapid changes that occur when two oppositely moving vortex rings of equal diameters collide (e.g. Schultz-Grunow 1981). Irrespective of the validity of the collision hypothesis, the limited flow visualization, using schlieren photography, that we carried out indicated that instability, roll-up and breakdown of the shear-layer structures occurred in a symmetric fashion. Similar observations were made by Rockwell & Niccolls (1973) and more recently by Hussain (1983).

The turbulence intensities on the centreline, normalized by U_0 or T_0, can give an indication of the start of the self-preserving region downstream of the interaction region. This is demonstrated in figure 6, which shows θ' and the r.m.s. of the three fluctuating velocity components u', v' and w'. Approximate self-preservation is established at $x/d \approx 20$. Similar results for θ' and u' were obtained by Pascal (1978), and have been included in figure 6. The u', v' and w' results of Krothapalli *et al.* (1981) have also been included. The u' distribution of Krothapalli *et al.* shows a small peak near $x/d = 12$, as in the present data, but this peak is not discernible in Pascal's u' distribution. It is possible, but not fully confirmed, that the nature of the centreline u'/U_0 curve depends on the nature of the boundary layers at the nozzle lips. If these are turbulent then a monotonic increase in u'/U_0 occurs (e.g. Hill, Jenkins & Gilbert 1976; and possibly Pascal 1978) while if they are laminar then a peak is observed (Hill *et al.* 1976; Krothapalli *et al.* 1981; and the present results). For the experiment of Weir *et al.* (1981) the initial boundary layers were laminar, but there is no discernible peak in their distributions of u'/U_0 and v'/U_0. Turbulent boundary layers at the nozzle lips may also account for the θ' peak of Pascal being smaller than the present peak. Another explanation of the difference in the u'/U_0 curves is related to the possibility that in Pascal's jet and the jet of Weir *et al.* (1981) the structures in

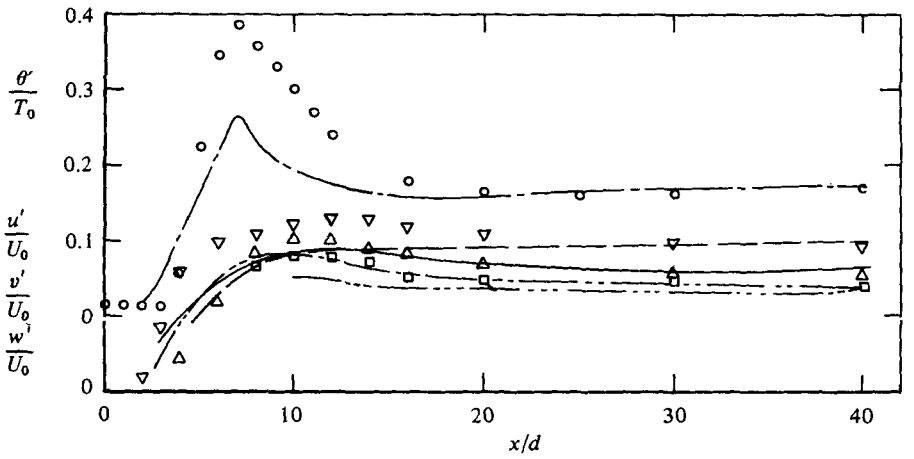

FIGURE 6. R.m.s. values of velocity and temperature fluctuations on the centreline of the jet. Present: ○, θ'/T_0; ▽, u'/U_0; △, w'/U_0; □, v'/U_0. Pascal (1978): — — —, θ'/T_0; — —, u'/U_0. Krothapalli *et al.* (1981): ——, u'/U_0; — — — —, v'/U_0; — — — — —, w'/U_0. Upper origin for ordinate is for θ'/T_0. Lower origin refers to u'/U_0, v'/U_0, w'/U_0.

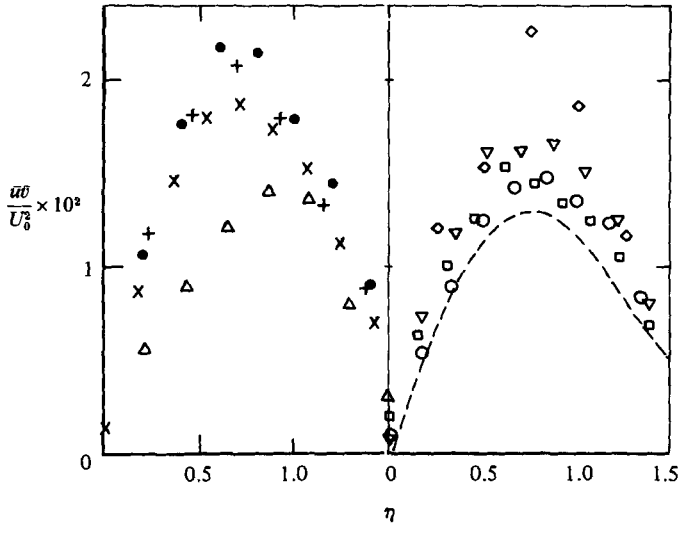

FIGURE 7. Reynolds shear-stress distributions across the jet. — —, Krothapalli *et al.* (1981), $x/d = 40$. Other symbols are as in figures 2 and 4.

the opposite mixing layers were, unlike the present jet, asymmetric with respect to the centreline. Both types of structures have been observed in the near region of a plane jet (a discussion of this is given in Antonia *et al.* 1983*b*). While it is not clear what causes a particular disposition, whether symmetric or asymmetric, of structures in the mixing layers,† it can easily be imagined that the interaction of asymmetric structures will not result in as major a redistribution of turbulence quantities as when the structures are symmetric.

† Hussain (1983) reports flow-visualization observations for an initially laminar plane jet that issues either from a 96:1 contraction or from the end of a duct attached to a nozzle. In the latter case the opposite shear layers tended to roll up into asymmetric structures. In the former the symmetric mode appeared to dominate.

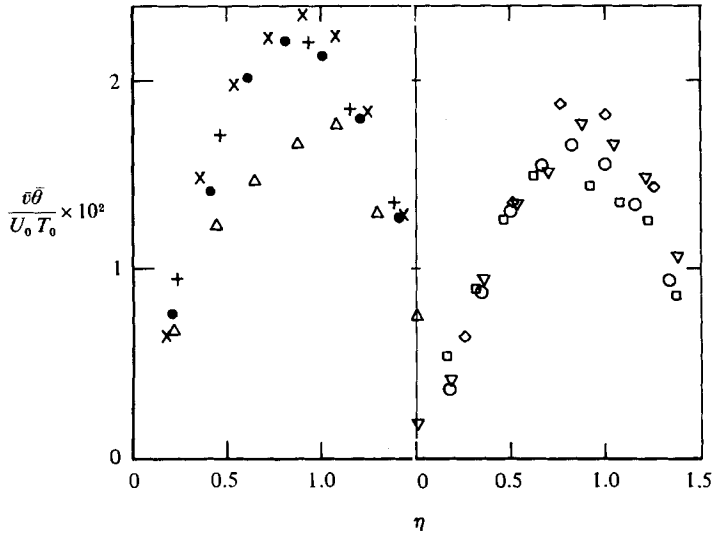

FIGURE 8. Heat-flux distributions across the jet. Symbols are as in figures 2 and 4.

The only other result for θ' in a plane jet that we have been able to find is that of Sunyach & Mathieu (1969). For their flow θ'/T_0 increases rapidly for $x/d > 3$, reaches a peak at $x/d = 7$ and then remains constant up to $x/d = 10$, the largest value considered in their experiment.

The Reynolds shear stress $\overline{uv}$ normalized by U_0^2 (figure 7) also shows the redistribution due to the encounter of the mixing-layer structures and the generation of the 'new' asymmetric structures. The origin of these latter structures was estimated to be at about $x/d \approx 12$ (Antonia *et al.* 1983*b*). This is approximately the location where the maximum value of $\overline{uv}$ occurs and where the centreline values of u'/U_0 and v'/U_0 peak. Similarly the turbulent heat flux $\overline{v\theta}/U_0 T_0$ (figure 8) has a maximum at $x/d = 7$, the same point where the θ'/T_0 centreline curve reaches a maximum. Both distributions assume small values at $x/d = 5$, increase rapidly to their peak values and then decrease, less rapidly, to the nearly self-preserving values at $x/d \approx 20$.

The $\overline{uv}/U_0^2$ distribution obtained by Krothapalli *et al.* (1981) for the nearly self-preserving region is in reasonable (figure 7) agreement with the present distributions at $x/d = 20$ and 40. When the maximum values of $\overline{uv}/U_0^2$ and $\overline{v\theta}/U_0 T_0$ are plotted (figure 9) as functions of x, the resulting distributions are qualitatively similar to those in figure 5.

6. Comparison with results of Weir *et al.* (1981)

An appropriate check was made of the 'timesharing' superposition analysis introduced by Bradshaw *et al.* (1973) when considering the interaction of boundary layers in a duct flow. Weir *et al.* (1981) reported good agreement of the superposition analysis for the plane jet while noting that the structures in either mixing layer did not quite timeshare near the centreline 'as simply as they appear to do in the duct'. To check the superposition procedure for the present flow, we used the self-preserving mixing-layer profiles for $\overline{q^2}$ at $x/d = 4$. The self-preserving development of each mixing layer in isolation was assumed using the coordinate y_1/x. Near the centreline the calculations overestimated measured values of $\overline{q^2}$ by a factor of about 2 at

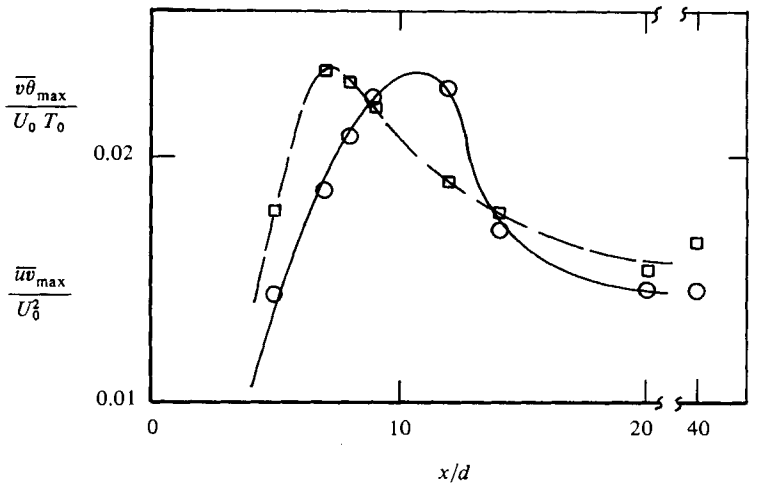

FIGURE 9. Streamwise variation of maximum values of Reynolds shear stress and lateral heat flux: ○, $\overline{uv}_{max}/U_0^2$; □, $\overline{v\theta}_{max}/U_0 T_0$.

$x/d = 10$ and about 10 at $x/d = 20$. For $\overline{\theta^2}$ the corresponding ratios for calculated to measured values are about 4 and 30 respectively.

The inappropriateness of the superposition procedure to the present flow is in contrast to the satisfactory use of the procedure by Weir *et al.* (1981). The difference ΔU between the mean velocity inferred from an assumed self-preserving development of the mixing layers and the measured local mean velocity is compared in figure 10 with the difference calculated by Weir *et al.*, using the superposition procedure for their flow. The difference between the measured value of ΔU in the present flow and the calculation of Weir *et al.* is not startling. Each set of curves in figure 10 suggests a similar evolution of $\Delta U/U_j$ throughout the interaction region. A possible lengthscale y_i for the interaction region is provided by the value of y at which $\Delta U \approx 0$. The present mean-velocity data in the range $7 < x/d < 20$ suggest that $y_i/d \approx 0{\cdot}17x/d - 1$. This lengthscale is significantly larger than that ($y_i/d \approx 0{\cdot}075x/d - 0.5$) inferred from the mean-velocity data of Weir *et al.* The use of y_i, together with a suitable scale for ΔU (e.g. the value U_i of ΔU at $y = 0$) would bring into agreement all the results of figure 10 when plotted in the form $\Delta U/U_i$ versus y/y_i. The validity of scales such as U_i and y_i† is not, however, supported by the results of figure 11. The measured difference $\Delta\tau$ between the value of $\overline{uv}$ inferred from an assumed self-preserving development of the mixing layers and the measured value of $\overline{uv}$ differs considerably from the calculation of $\Delta\tau$ reported by Weir *et al.* Negative values of $\Delta\tau$ are deduced from the present measurements in the range $5 \lesssim x/d \lesssim 10$, since large local values of $\overline{uv}$, in excess of those in the mixing layer, occur near the start of the interaction region. The present distributions of $\Delta\tau$ at $x/d = 12, 14, 20$ are positive but qualitatively very different from those calculated by Weir *et al.*

The inappropriateness of the superposition concept to the present flow reflects the strong interaction that occurs downstream of the potential core. We conjecture that the weaker interaction observed by Weir *et al.* was probably a result of the asymmetric arrangement of the mixing-layer structures with respect to the centreline.

† As noted earlier in the context of the relevance of U_0 and L_u in the interaction region, the mean velocity is an insensitive indicator of similarity.

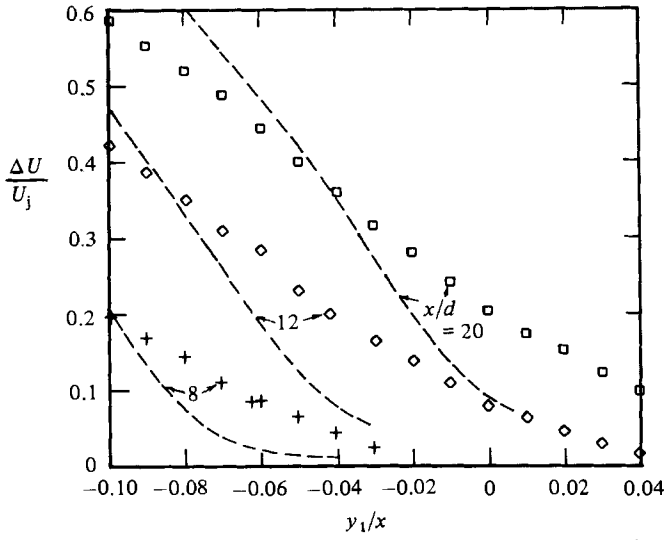

FIGURE 10. Departures of mean velocity from self-preserving mixing-layer distribution. Present measurements: +, $x/d = 8$; ◇, 12; □, 20. — —, calculated by Weir *et al.* (1981).

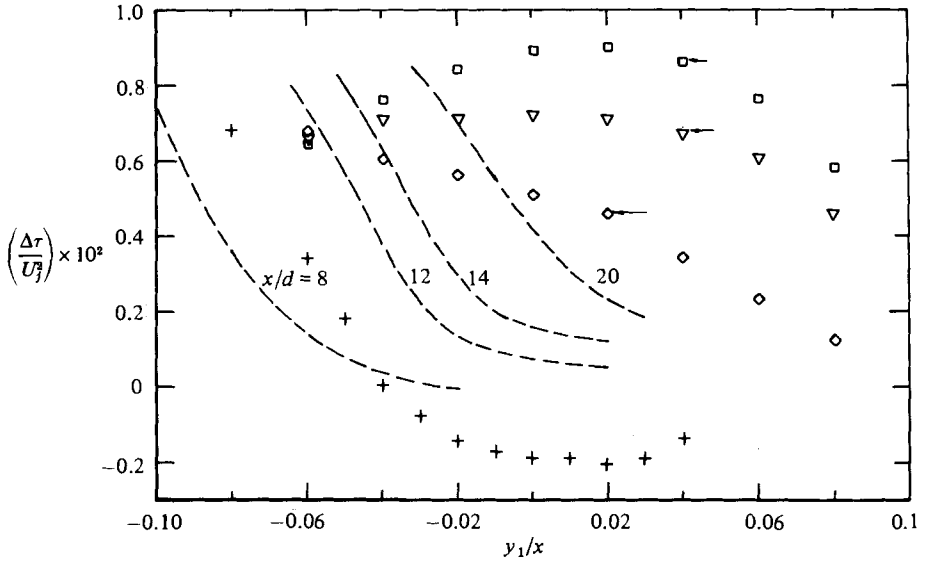

FIGURE 11. Departures of Reynolds shear stress from self-preserving mixing-layer distribution. Present measurements: +, $x/d = 8$; ◇, 12; ▽, 14; □, 20. — —, calculated by Weir *et al.* (1981).

Weir & Bradshaw (1975) had earlier documented evidence of oscillatory flapping† in the initial region of a plane jet issuing from the same contraction as used by Weir *et al.* If the flapping motion is associated with the presence of asymmetric structures, it is unlikely that the interaction would be as violent as when symmetric structures are present. In Rockwell & Niccolls' (1972) flow visualization a severe deformation of the potential core accompanied the symmetric mode of vortex growth, whereas the asymmetric mode caused the core to be only slightly disturbed.

† Weir & Bradshaw found a negative correlation coefficient between velocity fluctuations measured at $y = \pm\frac{1}{2}d$ over the range $0 < x/d \lesssim 16$.

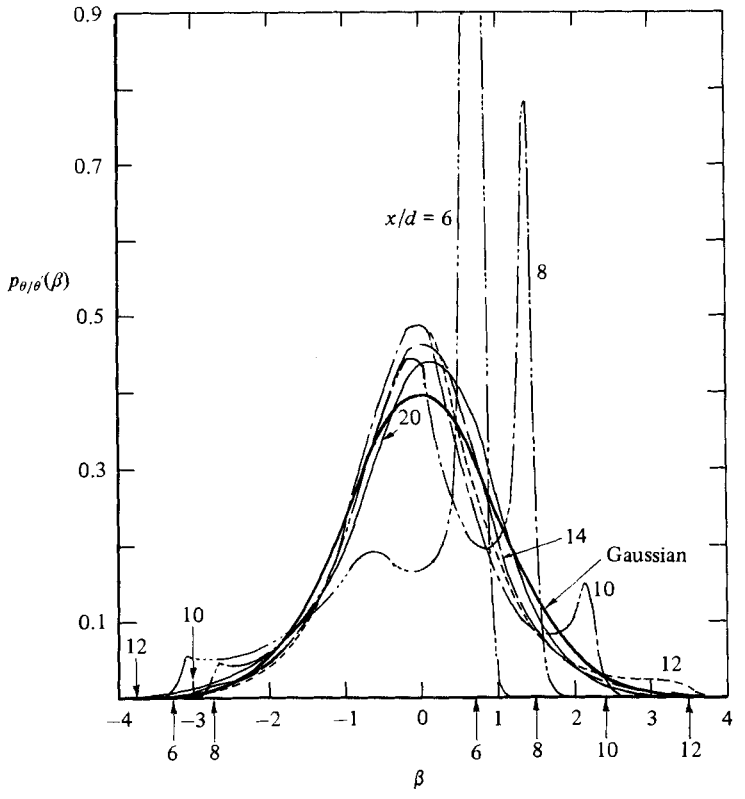

FIGURE 12. Evolution of the measured probability density function of temperature on the centreline of the jet.

7. Probability density functions, skewness and flatness

The evolution of the probability density function (p.d.f.) of temperature on the centreline of the jet also exhibits interesting characteristics (figure 12). At $x/d = 6$ the p.d.f. $p_{\theta/\theta'}$, defined such that $\int_{-\infty}^{\infty} p_{\theta/\theta'}(\beta)\,\mathrm{d}\beta = 1$, is dominated by the large peak that occurs near the core temperature. The parameter β represents the values in probability space that the normalized quantity θ/θ' can assume. The value of β corresponding to the jet temperature $(T_j - T)/\theta'$ (recall that both T_j and T are measured relative to the ambient temperature) is indicated by an arrow in figure 12. The value corresponding to the ambient temperature, $-T/\theta'$, is also denoted by an arrow. Ideally, a delta function would be expected at these two locations; in practice, the width of the spike observed reflects contributions from the noise of the electronics and from variations in the ambient temperature or the jet temperature. The p.d.f. is trimodal at $x/d = 6$, and retains this characteristic until at least $x/d = 10$. The magnitude of the peak that occurs near $\beta = 0$ first increases up to $x/d \approx 12$ and then decreases slightly at larger values of x. At $x/d = 20$, where the flow is approximately self-preserving, there is no evidence of a spike corresponding to the ambient temperature, implying no intrusion of 'irrotational' room fluid at the centreline at this location.

The persistence at the centreline of temperature excursions which can reach the jet temperature, for values of x/d up to 10, well beyond the potential core, seems surprising and requires an explanation. It has already been suggested that turbulence

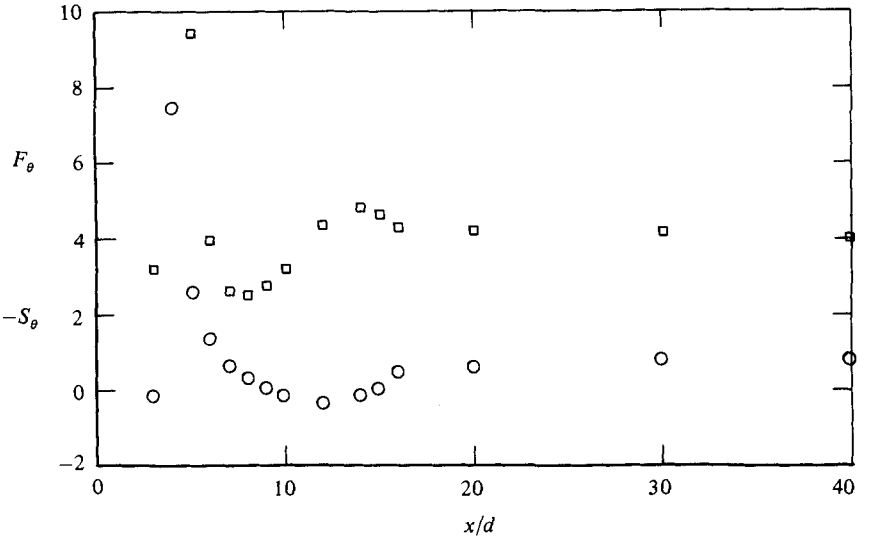

FIGURE 13. Variation of skewness and flatness factors of temperature on the centreline of the jet: ○, $-S_\theta$; □, F_θ.

quantities redistribute dramatically in the interaction region owing to the encounter of the symmetric mixing-layer structures. It seems reasonable to surmise that these structures, carrying with them parcels of core fluid at the exit jet temperature, will, when they meet, distribute such core fluid in a random way so that occasionally such fluid exists at the centreline. Molecular diffusion would ensure that this pattern did not persist for too long. Indeed at $x/d \approx 12$ the influence of these structures is no longer felt, as space–time correlations reported in Antonia *et al.* (1983*b*) indicated that this location coincided approximately with the onset of the new asymmetric structures.

As in the case of θ', the skewness S_θ ($\equiv \overline{\theta^3}/\theta'^3$) and the flatness factor F_θ ($\equiv \overline{\theta^4}/\theta'^4$) of θ do not approach their self-preserving values monotonically (figure 13). The distributions in figure 13 exhibit several interesting features. At $x/d > 20$ the magnitude of S_θ and F_θ on the centreline indicate that the temperature fluctuation is not Gaussian.† At $x/d = 3$ nearly Gaussian values are measured for S_θ and F_θ on the centreline, consistent with the expected Gaussian nature of temperature fluctuations at the nozzle exit. Near the end of the potential core the very large values registered for S_θ and F_θ reflect, as noted previously, occasional intrusions at the centreline of ambient-temperature fluid. In the interaction region the skewness on the centreline changes sign twice. Each change of sign corresponds approximately with an extremum in the flatness factor F_θ (a minimum at $x/d \approx 8$ and a maximum at $x/d \approx 14$). Antonia, Chambers & Elena (1983) noted that turbulent free shear flows and wall shear flows exhibit at least one location where the p.d.f. of θ is symmetrical but non-Gaussian. They referred to such locations as points of symmetry. In the present flow both the fifth and seventh order of moments of θ change sign at $x/d = 8$ and $x/d \approx 14$, but the p.d.f. of θ is symmetrical (figure 12) only at $x/d \approx 14$. The

† A negative value of S_θ of comparable magnitude has also been obtained in the self-preserving region of a wake (e.g. LaRue & Libby 1974; Sreenivasan 1981; Fabris 1983). This negative value may be caused by the tendency of the negative tail of $p_{\theta/\theta'}$ to approach the ambient temperature limit without actually reaching it.

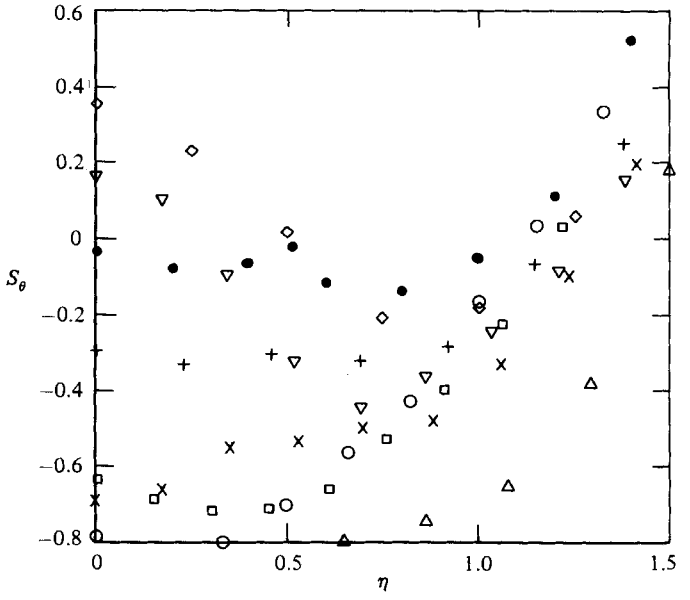

FIGURE 14. Distributions of temperature skewness S_θ across the jet. Symbols are as in figures 2 and 4.

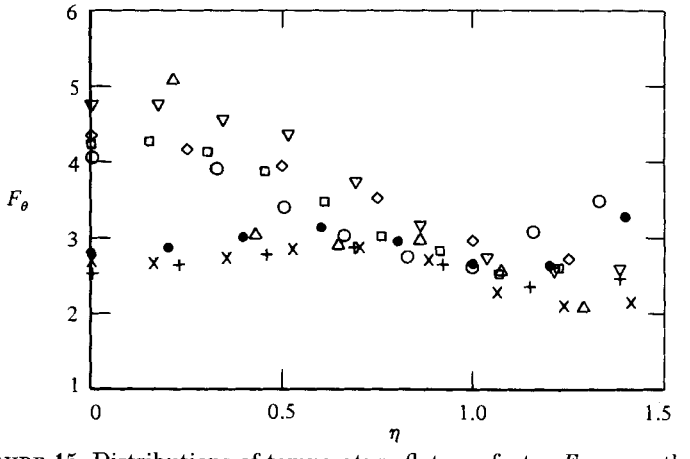

FIGURE 15. Distributions of temperature flatness factor F_θ across the jet. Symbols are as in figures 2 and 4.

p.d.f. of θ is also non-Gaussian at this location, as evidenced by the values of the flatness factor and higher even-order moments (not reported here) of θ. The behaviours of S_θ and F_θ away from the centreline are indicated in figures 14 and 15 respectively. Although there is streamwise variation at all η except near $\eta = 1$, the major streamwise variations occur, especially for S_θ, on the jet centreline. The distributions of S_θ and higher odd-order moments indicate that $p_{\theta/\theta'}$ is approximately symmetrical at η near 1.1.

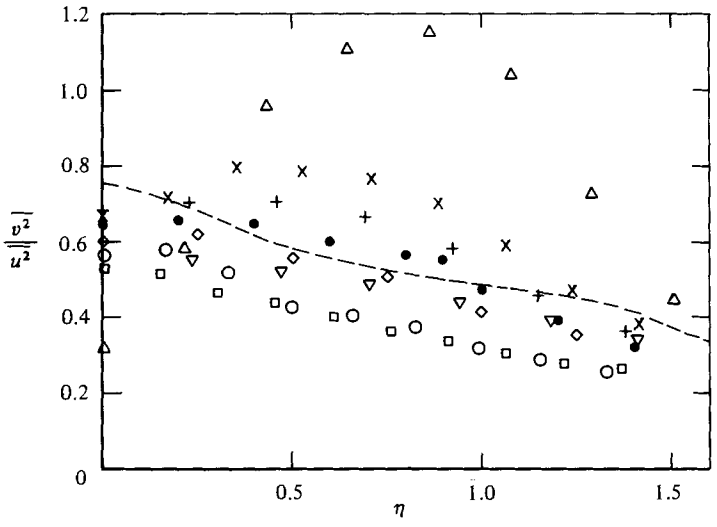

FIGURE 16. Distributions across the jet of the ratio of normal Reynolds stresses. Symbols are as in figures 2 and 4. — —, Krothapalli *et al.* (1981), $x/d = 40$.

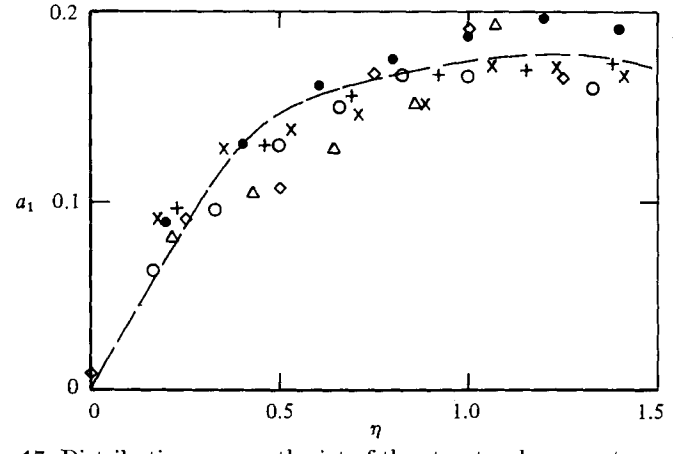

FIGURE 17. Distributions across the jet of the structural parameter a_1. Symbols are as in figures 2 and 4. — —, Krothapalli *et al.* (1981), $x/d = 40$.

8. Other turbulence structural parameters and turbulent Prandtl number

The skewness and flatness factors discussed in §7 are examples of turbulence structural parameters. We now consider other such parameters as well as the turbulent Prandtl number. It has been suggested (Murlis, Tsai & Bradshaw 1982) that $\overline{v^2}/\overline{u^2}$ represents a crude measure of the efficiency of turbulence mixing or of the 'coherence of turbulent eddies'. In contrast with the distributions of S_θ or F_θ (figure 13), the change in $\overline{v^2}/\overline{u^2}$ is relatively small on the centreline. More significant changes occur away from the centreline (figure 16), the ratio $\overline{v^2}/\overline{u^2}$ decreasing from a peak value of approximately 1.1 at $x/d \approx 5$ to values smaller than 0.5 at $x/d = 40$. This trend is consistent with the strongly coherent structures of the mixing layers and a decline in coherence with downstream distance.

The turbulence structural parameter $a_1 = \overline{uv}/\overline{q^2}$ does not change significantly throughout the interaction region (figure 17), suggesting that a unique prescription

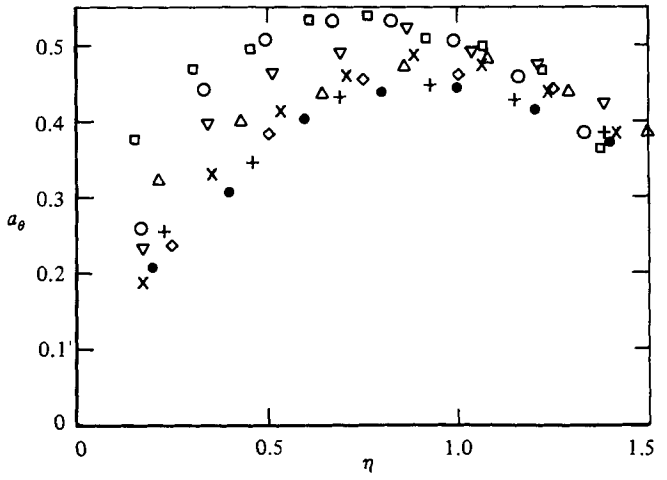

FIGURE 18. Distributions across the jet of the structural parameter a_θ. Symbols are as in figures 2 and 4.

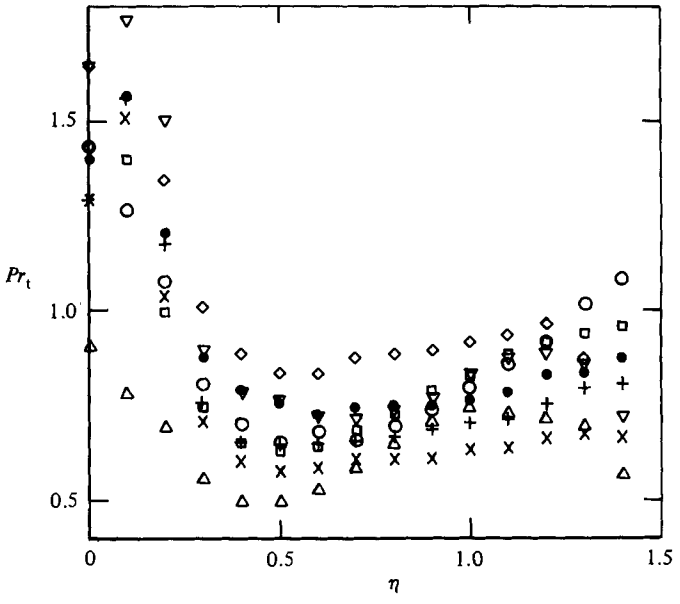

FIGURE 19. Distributions across the jet of turbulent Prandtl number Pr_t. Symbols are as in figures 2 and 4.

$a_1 = f(\eta)$ may be satisfactory for computational purposes. The maximum value of a_1 is in reasonable agreement with that obtained in other wall and free shear flows. There is reasonable agreement between the present values of a_1 at $x/d = 40$ and those obtained by Krothapalli *et al.* (1981) at $x/d = 40$. The structural parameter $a_\theta = \overline{v\theta}/(\theta'\overline{uv}^{\frac{1}{2}})$ can also be written as a combination of other structural parameters, e.g. $a_\theta = \rho_{v\theta}(\overline{v^2}/\overline{u^2})^{\frac{1}{4}}\rho_{uv}^{\frac{1}{2}}$, where $\rho_{\alpha\beta}$ is the correlation coefficient between fluctuations α and β. When expressed in this form, the variation with x/d of a_θ, shown in figure 18, reflects that of $\rho_{v\theta}$ and, to a lesser degree, that of $\overline{v^2}/\overline{u^2}$. The streamwise changes in a_θ seem more important than those for a_1, and would need to be taken into account in a heat-transfer calculation that makes use of a_θ.

To determine the turbulent Prandtl number Pr_t ($\equiv \overline{uv}(\partial T/\partial y)/\overline{v\theta}(\partial U/\partial y)$), the mean-velocity and mean-temperature gradients were obtained from curves of best fit through the data of figure 2. The results of figure 2 suggested that the same distribution for $\partial T/\partial y$ and $\partial U/\partial y$ would apply for $x/d \gtrsim 5$, and accordingly this distribution was used throughout the interaction region. The limiting values of Pr_t at $\eta = 0$ were inferred, using l'Hôpital's rule, from the behaviour of $\partial(\overline{uv}/U_0^2)/\partial\eta$ and $\partial(\overline{v\theta}/U_0T_0)/\partial\eta$ as η approaches zero. The changes in Pr_t (figure 19) are important near the origin. As in the case of $\overline{uv}/U_0^2$ and $\overline{v\theta}/U_0T_0$, Pr_t approaches its self-preserving distribution in a non-monotonic fashion. For example, at $\eta = 0.5$, Pr_t increases near the start of the interaction region to a maximum value (≈ 0.85) at $x/d \approx 11$ before decreasing to a self-preserving value of about 0.64. This behaviour mirrors that of $\overline{uv}_{max}/U_0^2$ more closely than that of $\overline{v\theta}_{max}/U_0T_0$ (figure 9). There is only a very narrow range of η, centred near $\eta = 0.5$, over which Pr_t could be claimed to be constant. It is pertinent to recall that Jenkins & Goldschmidt (1974) found that a conditional turbulent Prandtl number, accounting for intermittency in the region $\eta \gtrsim 1$, is significantly more constant† (≈ 0.4) than Pr_t.

9. Concluding remarks

The changes in the interaction region of the present jet are quite complex, and the reason for this may be attributed to the violent interaction between the symmetric mixing-layer structures. In the cylinder near wake, in the entrance region of a two-dimensional duct or in a plane jet with asymmetric mixing-layer structures, the interaction between opposite shear layers is unlikely to be as violent as in the present flow. It has been suggested (e.g. Krothapalli *et al.* 1981) that the presence or absence of a large centreline peak of u' in the jet interaction region may depend on the initial boundary layers on the nozzle lips being either laminar or turbulent. The evidence considered in this paper suggests that the large peak is more likely to be associated with the arrangement of the mixing-layer structures. It should also be noted that the r.m.s. temperature distribution immediately downstream of the potential core is a more sensitive indicator than u' or v' of the strength of the interaction between the shear layers.

The evolution, on the centreline, of probability density functions of temperature fluctuations and their associated moments, and the streamwise evolution of profiles of the Reynolds shear stress, average heat fluxes and turbulent Prandtl number indicate a non-monotonic approach to the state of self-preservation. It may be conjectured for the present jet that the approach towards approximate self-preservation starts at $x/d \approx 12$, this location coinciding approximately with the onset of the asymmetric structures which are more strongly in evidence in the nearly self-preserving region of the flow.

Although the change in a_1 is not appreciable, the variation in the ratio $\overline{v^2}/\overline{u^2}$ is significant, and suggests a decrease in the coherence of the self-preserving jet structures at $x/d \gtrsim 20$ compared with the mixing-layer structures. Structural parameters such as the skewness and flatness factors of θ and the parameter a_θ exhibit large changes, especially near the centreline. The turbulent Prandtl number Pr_t also varies appreciably throughout the interaction region. This variation should be taken into account in computer calculations for the interaction region. The centreline variation of the probability density function of temperature fluctuations should

† Possible causes for the difference between this value and the present values of Pr_t were discussed in Browne & Antonia (1983).

provide a useful input for calculations based on transport equations for the probability density function.

The large changes in the turbulence structure in the interaction region of the present jet preclude the application of the superposition procedure used by Weir *et al.* (1981). In the interaction region examined by the latter authors, the interaction was rather weak, probably because of the asymmetric arrangement about the centreline of the mixing-layer structures. From a modeller's viewpoint it is important that the experimenter's documentation of initial conditions includes a statement of whether the mixing-layer structures are symmetric or asymmetric with respect to the centreline.

The authors gratefully acknowledge the support of the Australian Research Grants Scheme.

REFERENCES

ABRAMOVICH, G. N. 1982 On the deformation of the rectangular turbulent jet cross-section. *Intl J. Heat Mass Transfer* **25**, 1885–1894.

ANTONIA, R. A., BROWNE, L. W. B., CHAMBERS, A. J. & RAJAGOPALAN, S. 1983*a* Budget of the temperature variance in a turbulent plane jet. *Intl J. Heat Mass Transfer* **26**, 41–48.

ANTONIA, R. A., BROWNE, L. W. B., RAJAGOPALAN, S. & CHAMBERS, A. J. 1983*b* On the organized motion of a turbulent plane jet. *J. Fluid Mech.* **134**, 49–66.

ANTONIA, R. A., CHAMBERS, A. J. & ELENA, M. 1983 Points of symmetry in turbulent shear flows. *Intl Commun. Heat Mass Transfer* **10**, 395–402.

BRADBURY, L. J. S. 1965 The structure of a self-preserving turbulent plane jet. *J. Fluid Mech.* **23**, 31–64.

BRADSHAW, P. 1977 Effect of external disturbances on the spreading rate of a plane turbulent jet. *J. Fluid Mech.* **80**, 795–797.

BRADSHAW, P., DEAN, R. B. & MCELIGOT, D. M. 1973 Calculation of interacting turbulent shear layers: duct flow. *Trans. ASME* I: *J. Fluids Engng* **95**, 214–219.

BROWNE, L. W. B. & ANTONIA, R. A. 1983 Measurements of turbulent Prandtl number in a plane jet. *Trans. ASME* C: *J. Heat Transfer* **105**, 663–665.

BROWNE, L. W. B., ANTONIA, R. A., RAJAGOPALAN, S. & CHAMBERS, A. J. 1983 Interaction region of a two-dimensional turbulent plane jet in still air. In *Structure of Complex Turbulent Shear Flow* (ed. R. Dumas & L. Fulachier), pp. 411–419. Springer.

EVERITT, K. W. & ROBINS, A. G. 1978 The development and structure of turbulent plane jets. *J. Fluid Mech.* **88**, 563–583.

FABRIS, G. 1983 Higher-order statistics of turbulent fluctuations in the plane wake. *Phys. Fluids* **26**, 1437–1445.

FLORA, J. J. & GOLDSCHMIDT, V. W. 1969 Virtual origins of a free plane turbulent jet. *AIAA J.* **7**, 2344–2346.

FOSS, J. F. & JONES, J. B. 1968 Secondary flow effects in a bounded rectangular jet. *Trans. ASME* A: *J. Basic Engng* **90**, 241–248.

GOLDSCHMIDT, V. W. & BRADSHAW, P. 1981 Effects of nozzle exit turbulence on the spreading (or widening) rate of plane free jets. *ASME Paper* 81-FE-22.

GOLDSCHMIDT, V. W., MOALLEMI, M. K. & OLER, J. W. 1983 Structures and flow reversal in turbulent plane jets. *Phys. Fluids* **26**, 428–432.

GUTMARK, E. & WYGNANSKI, I. 1976 The planar turbulent jet. *J. Fluid Mech.* **73**, 465–495.

HESKESTAD, G. 1965 Hot-wire measurements in a plane turbulent jet. *Trans. ASME* E: *J. Appl. Mech.* **32**, 721–734.

HILL, W. G., JENKINS, R. C. & GILBERT, B. L. 1976 Effects of the initial boundary-layer state on turbulent jet mixing. *AIAA J.* **14**, 1513–1514.

HUSSAIN, A. K. M. F. 1983 Coherent structures – reality and myth. *Phys. Fluids* **26**, 2816–2850.

HUSSAIN, A. K. M. F. & CLARK, A. R. 1977 Upstream influence on the near field of a plane turbulent jet. *Phys. Fluids* **20**, 1416–1426.

JENKINS, P. E. & GOLDSCHMIDT, V. W. 1974 A study of the intermittent region of a heated two-dimensional plane jet. *School Mech. Engng, Purdue Univ. Rep.* HL74-45.

KOTSOVINOS, N. E. 1975 A study of the entrainment and turbulence in a plane buoyant jet. Ph.D. thesis, California Institute of Technology.

KROTHAPALLI, A., BAGANOFF, D. & KARAMCHETI, K. 1981 On the mixing of a rectangular jet. *J. Fluid Mech.* **107**, 201–220.

LARUE, J. C. & LIBBY, P. 1974 Temperature fluctuations in the plane turbulent wake. *Phys. Fluids* **17**, 1956–1967.

MCGUIRK, J. J. & RODI, W. 1977 The calculation of three-dimensional turbulent free jets. In *Proc. Symp. on Turbulent Shear Flows, Pennsylvania State University*, vol. 1, pp. 1.29–1.36.

MOALLEMI, M. K. & GOLDSCHMIDT, V. W. 1981 Smoke wire visualization of the external region of a two-dimensional jet. In *Proc. 7th Biennial Symp. on Turbulence, University of Missouri–Rolla*, pp. 42-1–42-10.

MUMFORD, J. C. 1982 The structure of the large eddies in fully developed turbulent shear flows. Part 1. The plane jet. *J. Fluid Mech.* **118**, 241–268.

MURLIS, J., TSAI, H. M. & BRADSHAW, P. 1982 The structure of turbulent boundary layers at low Reynolds numbers. *J. Fluid Mech.* **122**, 13–56.

OLER, J. W. & GOLDSCHMIDT, V. W. 1981 Coherent structures in the similarity region of two-dimensional turbulent jets. In *Proc. 3rd Symp. on Turbulent Shear Flows, University of California, Davis*, pp. 11.1–11.6.

OLER, J. W. & GOLDSCHMIDT, V. W. 1982 A vortex-street model of the flow in the similarity region of a two-dimensional free turbulent jet. *J. Fluid Mech.* **123**, 523–535.

PASCAL, A. 1978 Contribution à l'étude d'un jet plan turbulent faiblement chauffé en écoulement incompressible. Thèse Docteur–Ingénieur, Institut National Polytechnique de Toulouse.

QUINN, W. R., POLLARD, A. & MASTERS, G. F. 1983 Measurements in a turbulent rectangular free jet. In *Proc. 4th Symp. on Turbulent Shear Flows, Karlsruhe, F.R. Germany*, pp. 7.1–7.6.

ROCKWELL, D. O. & NICCOLLS, W. O. 1972 Natural breakdown of planar jets. *Trans. ASME* D: *J. Basic Engng* **94**, 720–730.

SCHULTZ-GRUNOW, F. 1981 Generation of spatial turbulent spots. In *Proc. 7th Biennial Symp. on Turbulence, University of Missouri–Rolla*, pp. 52-1–52-4.

SFEIR, A. A. 1979 Investigation of three-dimensional turbulent rectangular jets. *AIAA J.* **17**, 1055–1060.

SFORZA, P. M. & STASI, W. 1979 Heated three-dimensional turbulent jets. *Trans. ASME* C: *J. Heat Transfer* **101**, 353–358.

SREENIVASAN, K. R. 1981 Evolution of the centreline probability density function of temperature in a plane turbulent wake. *Phys. Fluids* **24**, 1232–1234.

SUNYACH, M. & MATHIEU, J. 1969 Zone de mélange d'un jet plan: fluctuations induites dans le cône à potentiel–intermittence, *Intl J. Heat Mass Transfer* **12**, 1679–1697.

TENNEKES, H. & LUMLEY, J. L. 1972 *A First Course in Turbulence*. MIT Press.

TRENTACOSTE, N. P. & SFORZA, P. M. 1967 Further experimental results for three-dimensional free jets. *AIAA J.* **5**, 885–891.

WEIR, A. D. & BRADSHAW, P. 1975 Resonance and other oscillations in the initial region of a plane turbulent jet. *Dept Aeronautics, Imperial Coll. IC Aero. Rep.* 75-07.

WEIR, A. D., WOOD, D. H. & BRADSHAW, P. 1981 Interacting turbulent shear layers in a plane jet. *J. Fluid Mech.* **107**, 237–260.